Published in final edited form as:
Int J Cancer. 2010 March 15; 126(6): 1339–1352. doi:10.1002/ijc.24859.

Stromal cell-derived CSF-1 blockade prolongs xenograft survival of CSF-1-negative neuroblastoma

Dietmar Abraham[1], **Karin Zins**[1], **Mouldy Sioud**[2], **Trevor Lucas**[1], **Romana Schäfer**[1], **E. Richard Stanley**[3], and **Seyedhossein Aharinejad**[1]

[1] Laboratory for Cardiovascular Research, Vienna Medical University, Vienna, Austria

[2] Department of Immunology, The Norwegian Radium Hospital, Oslo, Norway

[3] Department of Developmental and Molecular Biology, Albert Einstein College of Medicine, New York, NY

Abstract

The molecular mechanisms of tumor–host interactions that render neuroblastoma (NB) cells highly invasive are unclear. Cancer cells upregulate host stromal cell colony-stimulating factor-1 (CSF-1) production to recruit tumor-associated macrophages (TAMs) and accelerate tumor growth by affecting extracellular matrix remodeling and angiogenesis. By coculturing NB with stromal cells *in vitro*, we showed the importance of host CSF-1 expression for macrophage recruitment to NB cells. To examine this interaction in NB *in vivo*, mice bearing human CSF-1-expressing SK-N-AS and CSF-1-negative SK-NDZ NB xenografts were treated with intratumoral injections of small interfering RNAs directed against mouse CSF-1. Significant suppression of both SK-N-AS and SK-N-DZ NB growth by these treatments was associated with decreased TAM infiltration, matrix metalloprotease (MMP)-12 levels and angiogenesis compared to controls, while expression of tissue inhibitors of MMPs increased following mouse CSF-1 blockade. Furthermore, Tie-2-positive and -negative TAMs recruited by host CSF-1 were identified in NB tumor tissue by confocal microscopy and flow cytometry. However, host-CSF-1 blockade prolonged survival only in CSF-1-negative SK-N-DZ NB. These studies demonstrated that increased CSF-1 production by host cells enhances TAM recruitment and NB growth and that the CSF-1 phenotype of NB tumor cells adversely affects survival.

Keywords

tumor–stromal cell interactions; xenograft models; growth factors and receptors; neuroblastoma

Neuroblastomas (NBs) are highly vascularized tumors that account for nearly 15% of all pediatric oncology deaths.[1] The molecular pathways determining poor outcome as well as the point of switch to poor prognosis are largely unknown.[2] The genetic aberration most consistently associated with poor outcome in NB is MYCN, a prominent oncogene that is a primary drug target in 22% of NB cases.[3–5] Although other major oncogenic pathways governing human neoplasia do not seem to be deregulated in NB,[6] multiple genes from several discrete genomic regions appear to be involved in NB tumorigenesis and

Correspondence to: Seyedhossein Aharinejad, Laboratory for Cardiovascular Research, Center for Anatomy and Cell Biology, Vienna Medical University, Waehringerstrasse 13, A-1090 Vienna, Austria, Fax: +431-4277-61120, seyedhossein.aharinejad@meduniwien.ac.at.

The first two authors contributed equally to this work.

progression.[7] Expression of angiogenic factors such as vascular endothelial growth factor (VEGF), fibroblast growth factor-2 and platelet-derived growth factor by NB cell lines and tumors plays differential roles in NB angiogenesis and metastasis.[8–11]

In addition to the requirement for several tumorigenic mutational events, nonmalignant cell types within the tumor stroma play an essential supporting role in extracellular matrix (ECM) remodeling, neoangiogenesis and lymphangiogenesis to promote tumor spread.[12,13] Tumor-associated macrophages (TAMs) that are recruited to tumors by a wide range of chemokines and growth factors[14–17] are increasingly being considered as key elements of the stroma that promote tumor development and progression.[12,18,19] TAMs enhance tumor growth through paracrine circuits involving the production of colony-stimulating factor-1 (CSF-1) by tumor cells[20,21] or other host-derived stromal cells and by ECM-modulating functions, mediated by matrix metalloproteases (MMPs).[22–24] CSF-1 regulates macrophage differentiation and function through the CSF-1 receptor, also known as c-fms and CD115,[25–27] accelerates angiogenesis *in vivo*[28] and stimulates monocytes to secrete biologically active VEGF to promote angiogenesis.[29]

Our recent reports suggested that the paracrine loop between cancer cells and TAMs leads to enhanced invasiveness of breast and colon carcinoma.[17,30] However, whether NB cells participate in such a paracrine loop with TAMs and how CSF-1 production by NB cells influences tumor growth remains unknown. In our study, we have therefore addressed the role of tumor cell- and stromal cell-derived CSF-1 in NB by studying CSF-1-expressing SK-N-AS and CSF-1-negative SK-N-DZ NB cell lines *in vitro* and *in vivo*.

Material and methods

Cell lines and molecular profiling

Mouse macrophages (CRL-2470) were obtained from American Type Culture Collection (ATCC, Manassas, VA) and cultured in Dulbecco's modified Eagle's medium (DMEM; Life Technologies, Rockville, MD) supplemented with 10% fetal calf serum (FCS; Invitrogen, Carlsbad, CA), 0.1 M nonessential amino acids (PAA Laboratories, Pasching, Austria), 100 U/ml penicillin, 100 μg/ml streptomycin (culture medium) and 10% L-929 fibroblast-conditioned medium containing mouse CSF-1.[31] Mouse S3T3 fibroblasts (CCL 92; ATCC) and the established human NB cell lines SK-N-AS (CRL-2137; ATCC) and SK-N-DZ (CRL-2149; ATCC) were propagated in culture medium.

Small interfering RNAs and analysis of their efficacy in vitro

Small interfering (si) RNAs directed against mouse CSF-1 (muCSF-1 si), human CSF-1 (CSF-1 si), human CSF-1 receptor (CSF-1R si) and scrambled siRNAs (scr si) were established and their efficacy examined *in vitro* by ELISA and real-time reverse transcription (RT)-PCR (Light Cycler; Roche, Mannheim, Germany) as described previously.[15] Based on activities determined *in vitro*, the optimal target sequences (from 3 tested) were as follows: muCSF-1 si: 5′-GACCCTCGAGTCAACAGAG-3′; CSF-1 si: 5′-GCCAAGATGTGGTGACCAA-3′; CSF-1R si: 5′-CCAG CAGCGTTGA TGTTAA-3′; and scr si: 5′-GGAACGATCTAGT CGACTC-3′. Only the sense strand sequences are shown. Chemically synthesized and purified siRNAs (Eurogentec, Philadelphia, PA) were used for all experiments as described previously.[15,32,33] To assess mouse CSF-1 siRNA efficiency, S3T3 fibroblasts were rinsed with PBS at 50% confluence, refed with serum-free DMEM and transfected with 100 nM muCSF-1 siRNA or scrambled siRNA in the presence of Lipofectamine (Invitrogen). Untreated cells served as controls. Specific inhibition of mouse CSF-1 but not human CSF-1 by mouse CSF-1 siRNA was tested in cocultures of human CSF-1-expressing SK-N-AS cells and mouse CSF-1-expressing fibroblasts and

macrophages. RNA was isolated (Trizol; Invitrogen) at different time points up to 96 hr following transfection for real-time RT-PCR. All experiments were performed in triplicate.

Cell proliferation assay

Human SK-N-AS and SK-N-DZ cells were seeded in 96-well plates at a density of 5×10^3 cells/well in culture medium. Cells were transfected with 100 nM human CSF-1 si (SK-N-AS only), human CSF-1R si or scrambled siRNA in the presence of Lipofectamine (Invitrogen). Twenty-four hours after transfection, the cells were kept in serum-free medium for 9 hr before stimulation with 3×10^3 U/ml CSF-1 (Chiron, Emeryville, CA) for 3 hr in serum-free DMEM. Additional controls were treated only with Lipofectamine alone to exclude transfection reagent-specific effects. Three hours following transfection or stimulation, DMEM containing FCS was added to a final volume of 100 μl containing 10% FCS. Triplicate cultures were maintained for an additional 24, 48 or 72 hr for each treatment. Cell proliferation was determined using the WST-1 reagent (Roche Diagnostics, Indianapolis, IN) according to the manufacturer's protocol.[34] Each experiment was repeated 3 times.

Coculture experiments

Human NB cells (2×10^5 cells/well) were cocultured with mouse macrophages (2×10^5 cells/well) and mouse fibroblasts (2×10^5 cells/well) in 6-well plates allowing direct cell–cell contact. Cells were allowed to adhere for 24 hr and then treated with 100 nM siRNA. Cocultures were treated with siRNA directed against mouse CSF-1. Three hours after transfection, cocultures were fed with DMEM supplemented with 1% FCS. Cells were incubated for 48 hr at 37° C before RNA isolation for real-time RT-PCR. Experiments were performed in triplicate.

Migration assay

NB cells alone (2×10^5 in 1 ml DMEM with 10% FCS) or NB cells mixed with mouse S3T3 fibroblasts (1×10^5 per cell line in 500 μl DMEM with 10% FCS) were seeded in 12-well plates. After cells had adhered, cocultures were transfected with 100 nM mouse CSF-1 siRNA or mouse VEGF siRNA using Lipofectamine 2000 according to the manufacturer's protocol or were left untreated. Twenty-four hours after transfection, macrophages (1×10^5 in 500 μl DMEM with 1% FCS) were added to the top of each Boyden migration chamber (8-μm, 12-well plate format; BD Biosciences, Palo Alto, CA). After 24 hr, the medium was removed and membranes were washed twice with PBS. Cells from the upper side of the membrane were removed with cotton swabs. The membranes were excised using a scalpel, inverted and transferred to a PBS-filled tissue culture well. Membranes were then fixed in methanol for 2 min at –20° C. After washing in PBS, membranes were stained with 1 μg/ml 4′-6-diamidino-2-phenylindole (DAPI) for 10 min at RT and washed again. Membranes were then embedded in Cityfluor (Cityfluor, Leicester, UK) on glass slides under coverslips. Representative sectors of migrated macrophages were counted under a fluorescence microscope. Each experiment was performed in triplicate.

Tumor models and siRNA treatment

The experiments performed in our study were approved by the Institutional Animal Care and Use Committee at the Vienna Medical University. Pathogen-free, male, 5-week-old athymic *nu/nu* (nude) mice (Harlan-Winkelmann, Borchen, Germany) were weighed, coded and divided into experimental groups of $n = 8$ at random. Mice were anesthetized (ketamine hydrochloride/xylazine at 55/7.5 mg/kg, i.p.) and 4×10^6 SK-N-AS or 8×10^6 SK-N-DZ cells/150 μl PBS were injected s.c. into the left flank.[15] The growth of the tumor xenograft was evaluated in a pilot study by determining the tumor weight every other day ($n = 24$; 12

animals/cell line). Ten days after cell injection, 1 group of animals was sacrificed and evaluated for tumor weight. Anesthetized mice received siRNAs against muCSF-1 to target stromal cell-derived CSF-1 and control animals received scrambled siRNA or Ringer's solution intratumorally or were untreated. Importantly, stromal cell-derived (mouse) CSF-1 does not activate human CSF-1R on cancer cells.[35,36]

Treatment was initiated on day 10 at a dose of 10 μg/injection and cycled every 3 days. The selected dosage of 10 μg/injection was based upon pilot studies in mice ($n = 24$; 12 mice/cell line). Tumor volumes were calculated as follows: (length × width^2)/2. All animals were sacrificed on day 24.

Analysis of the effects of CSF-1 blockade on survival

The survival study ($n = 40$) was set for 3 months. Mice were treated with muCSF-1 siRNA ($n = 8$), Ringer's solution ($n = 6$) or scrambled siRNA ($n = 6$) for each SK-N-AS and SK-N-DZ groups and were euthanized when moribund.

Analysis of the effects of CSF-1 blockade in vivo

On day 24, tumors were isolated, weighed and the animals were sacrificed. One portion of the tissue was processed for paraffin embedding and the remainder was processed for real-time RT-PCR, western blotting and radioimmunoassay (RIA),[14] as described later. Paraffin-embedded serial sections were rehydrated in graded alcohols and antigen retrieval was performed in a microwave in 0.1 M sodium citrate (pH 6.5). Following incubation in 5% H_2O_2 to block endogenous peroxidase activity, antigens were detected with Ki-67 antibody (tumor proliferation assay; Dako, Glostrup, Denmark), or a rabbit polyclonal von Willebrand Factor antibody (vWF; Abcam, Cambridge, UK), to evaluate the density of endothelial cells (ECs).[14,15] Macrophages were immunostained with anti-F4/80 rat monoclonal antibody (Caltag Laboratories, Burlingame, CA).[14,15,37] Primary antibodies were detected by sequential incubation with appropriate biotinylated secondary antibodies (Vector Laboratories, Burlingame, CA) and peroxidase-conjugated streptavidin (Dako), developed with 3,3′-diaminobenzidine (Vector Laboratories), counterstained with hemalaun, dehydrated and mounted in Entellan (Merck, Darmstadt, Germany). Digitalized images were generated and morphometry was carried out by counting the number of vWF-positive ECs or F4/80-positive cells in 10 consecutive (×20) fields per slide and results are expressed as cells/mm^2. Fluorescence labeling was performed on sections following antigen retrieval by sequential incubation with polyclonal rabbit anti-mouse Tie-2 (Santa Cruz Biotechnology, Santa Cruz, CA) antibody, polyclonal, multiple absorbed, TRITC-conjugated donkey anti-rabbit immunoglobulins (Jackson ImmunoResearch, West Grove, PA) and Alexa-488-conjugated rat monoclonal anti-mouse F4/80 antibody (Serotec, Oxford, UK). Sections were embedded in Cityfluor (City-fluor) and confocal images were captured on a Zeiss LSM-Meta microscope.

Mouse CSF-1 immunohistochemistry

Tumor tissue was snap frozen in liquid nitrogen and 5-μm cryosections were fixed in acetone for 8 min at 4° C, blocked and sequentially stained with polyclonal goat anti-mouse CSF-1 serum (Santa Cruz Biotechnology), biotin-conjugated horse anti-goat Ig (Vector Laboratories) and Alexa Fluor 488-conjugated streptavidin (Molecular Probes/Invitrogen, Carlsbad, CA) in PBS supplemented with 5% horse serum. Slides were then rinsed with PBS, counterstained in 0.1 μg/ml DAPI, mounted in Cityfluor (Cityfluor) and analyzed by fluorescence microscopy (Zeiss, Thornwood, New York).[38]

Fluorescence-activated cell sorting analysis

Tumors sections were rinsed in PBS supplemented with 0.3% bovine serum albumin and 0.1% sodium azide (staining buffer), minced, mechanically dissociated following collagenase digestion at 37° C for 30 min and passed through a 100-μm cell strainer. Erythrocytes were lysed in 155 mM NH_4Cl, 10 mM $KHCO_3$ and 0.1 mM EDTA (pH 8) for 10 min at 4° C. Cells were then washed in PBS and sequentially stained with biotinylated monoclonal rat anti-mouse Tie-2/CD202 (eBioscience, San Diego, CA), phycoerythrin-conjugated streptavidin (BD Biosciences, Franklin Lakes, NJ) and Alexa-488-conjugated monoclonal rat anti-mouse F4/80 (Serotec) in staining buffer for 30 min on ice in the presence of Fc block (BD Biosciences). Membrane-compromised cells were excluded with 7AAD (BD Biosciences) and 10^4 viable events analyzed on a FACscan flow cytometer (BD Biosciences) with an argon laser tuned to 488 nm.

Quantitative real-time RT-PCR

Tissue and cultured cells were processed for PCR as described previously.[14,15,39] The primer sequences for mouse molecules are as follows (sense/antisense): CSF-1: 5′-CATC TCCATTCCCTAA ATCAAC-3′/5′-ACTTGCTGATCCTCCT TCC-3′; CSF-1R: 5′-GCGATGTGTGAGCAATGGCA-3′/5′-CGGATAATCGAACCT CGCCA-3′; VEGF-A: 5′-TACTGC TGTACCTCCACC-3′/5′-GCT CATTCTCTCTATGTGCTG-3′; KDR: 5′-GGAGATTGAAAGA GGAAC-3′/5′-ACTTCCTC TTCCTCCATAC-3′; MMP-2: 5′-CCGATTATCCCATGAT GAC-3′/5′-ATTCCCTGCGAAGAACAC-3′; β-2 microglobulin: 5′-CCTCACATTGAAATCCAAATGC-3′/5′-CGGCCAT ACTGTCATGCTTAAC-3′. The primer sequences for human molecules are as follows (sense/antisense): CSF-1: 5′-GCT GTTGTTGGTCTGTCTC-3′/5′-CATGCTCTTCATAATCCTT G-3′; CSF-1R: 5′-TGCTGCTCCTGCTGCTATTG-3′/5′-TCAGCATCTT CACAGCCACC-3′; VEGF-A: 5′-AGAAGGAGGAGGGCAGAA TC-3′/5′-GCATTCACATTTGTTGTG CTG-3′; β-2 microglobulin: 5′-GATGAGTATGCCTGCCG TGTG-3′/5′-CAATCCAAATGCGG CATCT-3′. The specificity of the primers was tested by examining the melting curves of the products obtained using both human- and mouse-specific primers on RNA from both human and mouse cells as described previously.[16] Measurements were performed in triplicate.

CSF-1 RIA

Preweighed tissue samples were homogenized, heat-inactivated, centrifuged and the supernatant saved for assay as described previously.[31] CSF-1 was measured in duplicate on 3 samples from each mouse using a RIA that detects only biologically active mouse CSF-1.[31,40]

Western blotting

Tissue lysates were prepared and separated (50 lg/lane) by 8–12% SDS-PAGE prior to electrophoretic transfer onto Hybond C super (Amersham Pharmacia Biotech, Buckinghamshire, UK) as described elsewhere.[15] The blots were probed with polyclonal antibodies against MMP-2 (Chemicon, Temecula, CA), MMP-12 (Santa Cruz Biotechnology), TIMP-2 and TIMP-3 (Chemicon) before incubation with horseradish peroxidase-conjugated secondary antibodies (Amersham Pharmacia Biotech). Proteins were immunodetected by chemiluminescence (Supersignal-West-Femto; Pierce, Rockford, IL) and quantified by Easy Plus Win 32 software (Herolab, Wiesloch, Germany).

Statistical analysis

The Wilcoxon rank test was used to compare data between the groups. All statistical tests were 2-sided. The χ^2 test was used to compare the groups in long-term survival (3-month) analysis. The overall survival curves after treatment were analyzed by the Kaplan–Meier

survival test. Statistical tests were performed with the use of SPSS software (version 10.0.7; SPSS, Chicago, IL). Data are expressed as means ± SD. p values of <0.05 were considered to indicate statistical significance.

Results

CSF-1 is differentially expressed in growing NB cancer cells and host stromal cells

As CSF-1 production by cells within the tumor tissue can play a major role in macrophage recruitment to tumors and affect their growth, we studied whether cancer cell–stromal cell interactions affect the expression of human CSF-1 and its receptor (CSF-1R). We analyzed tumor tissue expression of CSF-1 and CSF-1R in human SK-N-AS and SK-N-DZ cancer cells and mouse stromal cells by using mouse- (host) and human-specific primers in quantitative real-time RT-PCR, when NB cells were xenografted to mice. Both SK-N-AS and SK-N-DZ cells expressed the human (hu) CSF-1R *in vivo*, which increased from day 10 to day 24. Likewise, host CSF-1R mRNA was expressed throughout tumor growth (Fig. 1*a*). In contrast, huCSF-1 mRNA expression was significantly downregulated in SK-N-AS cells over time, and SK-N-DZ cells did not express human CSF-1 mRNA at all. Importantly, host CSF-1 mRNA expression increased moderately in tumor tissue from day 10 to day 24 (Fig. 1*a*). In addition, specific host CSF-1 protein expression was detected by immunohistochemical staining with a mouse CSF-1-specific antibody at day 10 in the stromal cells of both SK-N-AS and SK-N-DZ tumors (Fig. 1*b*).

CSF-1 promotes SK-N-DZ proliferation but not SK-N-AS proliferation

To test whether CSF-1 promotes cancer cell proliferation, we first treated human NB cells with siRNAs directed against human CSF-1 (SK-N-AS only) or CSF-1R siRNA (both cell lines) or transfected the cells with scrambled siRNA and then stimulated them with recombinant CSF-1 protein and determined cell proliferation for up to 72 hr. CSF-1 did not promote SK-N-AS proliferation and CSF-1 or CSF-1R suppression did not reduce cell proliferation, compared to untreated control cells, Lipofectamine-treated cells or scrambled siRNA-transfected cells (Fig. 2*a*).

In contrast to the results obtained in SK-N-AS cells, SKN-DZ cell proliferation was significantly increased after 72 hr of incubation with recombinant CSF-1 and significantly decreased after inhibition of CSF-1R production or inhibition of CSF-1R and concomitant stimulation with recombinant CSF-1, compared to untreated control cells, Lipofectamine-treated cells or cells transfected with scrambled siRNA (Fig. 2).

These data indicate that CSF-1 promotes proliferation of CSF-1-negative SK-N-DZ but not CSF-1-positive SK-N-AS cells. The role of the CSF-1R in mediating CSF-1-stimulated proliferation of SK-N-DZ cells was tested by transfecting SKN-DZ with huCSF-1R siRNA and examining their response to recombinant human CSF-1. CSF-1R siRNA treatment abrogated the CSF-1 response, consistent with the proliferative effect of CSF-1 being mediated by the CSF-1R.

Tumor–stromal cell interaction increases stromal CSF-1 target gene expression

To assess whether the interaction between cancer cells and stromal cells regulates CSF-1 production in stromal cells such as fibroblasts and macrophages, thereby potentially affecting stromal cell gene expression and migration, we performed co-culture experiments of SK-N-AS or SK-N-DZ cancer cells with murine CRL-2470 macrophages and 3T3 fibroblasts treated with muCSF-1 si to analyze the role of stromal cell-derived CSF-1. Coculturing cancer cells with fibroblasts and macrophages significantly increased the mRNA expression of mouse CSF-1 and VEGF-A as compared to cultures of macrophages

and fibroblasts alone (Fig. 2*b*). Mouse MMP-2 levels, however, were only moderately changed. To determine the relation of these gene expression changes in stromal cells, we treated cocultured NB cancer cells, mouse fibroblasts and macrophages with siRNA specifically directed against mouse CSF-1. Inhibition of mouse CSF-1 in macrophages and fibro-blasts resulted in significantly decreased mRNA expression of mouse CSF-1 and VEGF-A but not MMP-2 compared to untreated cocultures of both SK-N-AS and SK-N-DZ cancer cells (Fig. 2*b*). In contrast, human CSF-1 mRNA levels from human CSF-1-expressing SK-N-AS cancer cells were not changed by coculturing and treatment with muCSF-1 si (Fig. 2*b*). This indicates that the muCSF-1 siRNA specifically inhibits mouse CSF-1 but not human CSF-1 production by cancer cells. Furthermore, these results suggest that the interaction between NB cancer cells and stromal cells leads to induction of stromal cell-derived CSF-1 and that CSF-1 in turn increases stromal cell expression of VEGF-A but not MMP-2.

Tumor–stromal cell interactions promote macrophage migration through stromal CSF-1 and VEGF-A

To analyze whether the observed changes in stromal cell-derived CSF-1 and VEGF-A levels induced by cancer cell– stromal cell interactions affect the recruitment of macrophages, we compared the effects of muCSF-1 si- and muVEGF si-treated cocultured fibroblasts and cancer cells on macrophage migration *in vitro*. Coculturing significantly increased macrophage migration compared to cultured cells alone or in cocultures of both NB cell lines. Recruitment activity was however much higher in cocultured SK-N-AS cells compared to cocultured SK-N-DZ cells (Figs. 2*c* and 2*d*). Treatment with muCSF-1 siRNA and to a similar extent with muVEGF-A siRNA significantly reduced macrophage migration, indicating a role for stromal cell-derived CSF-1 and VEGF-A in the recruitment of macrophages (Figs. 2*c* and 2*d*).

Host CSF-1 blockade suppresses NB growth

The CSF-1 expression data suggest that stromal cells are a constant source of CSF-1 in NB growth and that human CSF-1 produced by SK-N-AS but not SK-N-DZ cells could also contribute to the level of CSF-1. To analyze whether stromal cell-derived CSF-1 in NBs plays a critical supporting role for the overall growth of the tumor, tumor bearing mice were treated with muCSF-1 siRNA (specifically targeting mouse but not human CSF-1 mRNA), scrambled siRNA, Ringer's solution or were untreated. To assess treatment modalities *in vivo*, we initially assessed muCSF-1 siRNA transfection efficiency *in vitro*. Treatment of mouse S3T3 fibroblasts revealed a significant reduction in CSF-1 mRNA for up to 3 days (Fig. 2*e*). We therefore decided to cycle intratumoral muCSF-1 siRNA applications every 3 days to guarantee continuous reduction of stromal cell-derived CSF-1. At the beginning of treatment on day 10, mice developed human NB tumors of comparable size (SK-N-AS: 190 ± 36 mg and SK-N-DZ: 167 ± 39 mg; $p = 0.516$). The mean tumor weight was markedly reduced in mice with SK-N-AS NB treated with muCSF-1 siRNA (1,451 ± 595 mg) compared to mice treated with Ringer's solution (3,773 ± 640 mg), scrambled siRNA (4,388 ± 569 mg) or untreated control mice (4,180 ± 451 mg) (Fig. 3*a*). In mice bearing SK-N-DZ NB, the mean tumor weights were 3,452 ± 500 mg, 3,423 ± 444 mg and 3,165 ± 308 mg in the untreated, Ringer's solution-treated and scrambled siRNA-treated mice and declined significantly to 1,534 ± 225 mg in muCSF-1 siRNA treated mice (Fig. 3*a*). In the SK-N-AS NB mice therefore, treatment with muCSF-1 siRNA suppressed tumor growth by 65%, and in SK-N-DZ NB mice treatment with muCSF-1 siRNA suppressed tumor development by 56%. Interestingly, despite this growth advantage of SK-N-AS NBs, the mouse CSF-1 blockade resulted in a similar reduction in growth rate for both NB xenografts, that was already apparent at day 13, 3 days after the first muCSF-1 siRNA treatment at day 10 (Fig. 3*a*).

To analyze the long-term effect of host CSF-1-blockade on NB growth, we determined the effect on animal survival. In mice bearing human CSF-1 negative SK-N-DZ NB xenografts, the median time to death in both the Ringer's solution and scrambled siRNA control groups was 41 days, and all mice died between 41 and 46 days after tumor cell grafting. However, survival was significantly increased in mice following muCSF-1 siRNA treatment vs. control mice, and their median time to death was 46 days. At day 46 (at which time the last animal in the control groups died), 50% of muCSF-1 siRNA-treated mice were still alive (Fig. 3*b*). In contrast, there was no response to muCSF-1 siRNA treatment observed in mice bearing human CSF-1-positive SK-N-AS xenografts. The median time to death of mice in the Ringer's solution and scrambled siRNA control groups was 34 and 31 days, respectively, and all mice died between 31 and 36 days following tumor cell engraftment. The median survival time following muCSF-1 siRNA treatment was 34 days, and all mice died between 31 and 38 days (not significant *vs.* controls). Thus, while blockade of stromal cell CSF-1 expression significantly suppressed the growth of both human NB xeno-grafts, only the mice bearing CSF-1-negative SK-N-DZ tumors exhibited improved survival, indicating a negative role for tumor cell CSF-1 expression on survival.

Host CSF-1R expression is reduced after host CSF-1 blockade in SK-N-DZ but not in SK-N-AS NBs

To better understand the effect of host CSF-1 blockade, we measured host CSF-1 and CSF-1R expression in NB tissue in all experimental groups. Host muCSF-1 mRNA and protein expression increased with tumor growth in SK-N-AS and SK-N-DZ tumor lysates (Figs. 3*c* and 3*d*). With muCSF-1 siRNA treatment, day 24 tumor tissue muCSF-1 mRNA levels declined significantly compared to controls. Importantly, muCSF-1 siRNA treatment reduced host CSF-1 protein expression as detected by immunohistochemical staining with a mouse CSF-1-specific antibody in SK-N-AS tumors. Quantitative measurement of mouse CSF-1 protein by RIA confirmed this finding by showing significantly reduced mouse CSF-1 protein levels in SK-N-AS and SK-N-DZ tumor tissue following muCSF-1 siRNA treatment (Fig. 3d). muCSF-1R mRNA levels declined with muCSF-1 siRNA treatment in huCSF-1-negative SK-N-DZ but not huCSF-1-positive SK-NAS tumor lysates (Fig. 3*e*).

Recruitment of both Tie-2-positive and Tie-2-negative macrophage subpopulations is regulated by CSF-1

Following NB cell engraftment in mice, TAMs were detected within the tumor stroma (positive macrophage-specific F4/80 antibody staining). In both SK-N-AS and SK-N-DZ tumor tissue, the TAMs lined vascular channels, which were surrounded by tumor cells and contained blood cells (Fig. 4*a*). Treatment with muCSF-1 siRNA reduced macrophage recruitment to the tumor and reduced the density of these vascular channels and the number of lining TAMs in SK-NAS and SK-N-DZ xenografts (Fig. 4a). These experiments indicate that infiltrating CSF-1-dependent TAMs are associated with vascular channels in human SK-N-AS and SK-NDZ NB xenografts.

Confocal microscopy was used to further analyze the tissue distribution of recruited macrophages in CSF-1-positive SK-N-AS NB xenografts by using anti-F4/80 antibody and a Tie-2 antibody that primarily stains endothelial cells. F4/80-positive TAMs were visualized by green fluorescence and Tie-2-positive cells by red fluorescence. Tie-2^{+}F4/80^{+} TAMs are shown to colocalize with Tie-2-positive endothelial cells, indicating that F4/80-positive macrophages are preferentially recruited to vessels (Fig. 4*b*). However, these images also suggested that some F4/80-positive macrophages in these highly vascularized tumors lack expression of Tie-2.

To further characterize the TAMs in mice bearing human CSF-1-positive SK-N-AS NB xenografts and their response to treatment with muCSF-1 siRNA, we performed flow cytometry using F4/80 and Tie-2 antibodies. In tumor tissue of muCSF-1-treated mice, both F4/80-positive TAMs and Tie-2-positive cell numbers significantly decreased from 5% ± 1.7% and 4.7% ± 1.8% to 2.5% ± 0.9% (TAMs) and 10.8% ± 2.2% and 9.9% ± 2.6% to 5.3% ± 1.8% (Tie-positive cells) in control and scr si compared to muCSF-1 si treated tumors, shown representatively in Figure 4*c*. The number of Tie-2-positive TAMs also decreased by half from 3.7% ± 1.4% and 3.1% ± 1.2% to 1.9% ± 0.6% following treatment with muCSF-1-siRNA, respectively (Fig. 4*c*). These data indicate the presence of a Tie-2-positive TAM fraction in SK-N-AS NB tissue and also indicate that its presence is to a large extent dependent on CSF-1.

muCSF-1 blockade specifically upregulates TIMPs and downregulates TAM-specific MMP-12 in NB xenografts

In association with increased macrophage infiltration, the expression of host MMP-12, a macrophage-specific protease involved in ECM remodeling,[41] increased with tumor development in both SK-N-AS and SK-N-DZ control tumor lysates (Fig. 5). In addition, mouse MMP-2, a key molecule in tumor metastasis and angiogenesis,[42] was upregulated with tumor growth in control animals. muCSF-1 siRNA treatment significantly lowered the expression of the macrophage-specific MMP-12 without affecting tumor tissue levels of MMP-2 (Fig. 5). TIMP-2 and -3 protein expression in tumor lysates increased with tumor growth in control mice and muCSF-1 blockade resulted in a significant increase in their expression (Fig. 5). These experiments show that muCSF-1 blockade increases the expression of TIMP-2 and -3 in NB xenografts.

Host, but not cancer cell-derived VEGF-A, plays a key role in mediating the angiogenic activity of CSF-1

Immunocytochemistry of endothelial cell-specific vWF-stained sections conclusively showed increased angiogenesis in control NB xenografts. muCSF-1 siRNA treatment decreased endothelial cell density significantly compared to controls (Fig. 6*a*). Consistent with this finding, tumor tissue mRNA expression of host VEGF-A, and its receptor KDR, increased with tumor growth and decreased in muCSF-1 siRNA-treated but not in scrambled siRNA-treated SK-N-AS and SK-N-DZ mice (Fig. 6*b*). In contrast to mouse VEGF-A, human VEGF-A expression declined with tumor growth in both NB xenografts. Of note, while host-cell VEGF-A expression was suppressed by muCSF-1 siRNA treatment in both NB tumors, human VEGF-A expression was only suppressed in the CSF-1-negative SK-N-DZ tumors (Fig. 6*b*). As the suppression of EC numbers by CSF-1 blockade was similar in both tumors (Fig. 6*a*), it is likely that the contribution of human VEGF-A to angiogenesis up to day 24 is small. Thus, these data indicate that host cells are a major source of angiogenic factors in NB xenografts.

Discussion

In our study, we have used 2 NB xenograft models with different CSF-1 expression phenotypes to investigate the role of CSF-1 in the regulation of host TAMs that play a key role in the NB tumor stroma compartment.[12,14,15] In addition to the different CSF-1-phenotype, the NB cell lines used also differed with respect to their MYCN-genotype. The CSF-1-expressing SK-N-AS NB cell line displays no MYCN amplification,[43] whereas the CSF-1-negative SK-N-DZ cell line has high levels of MYCN.[44] These cell lines have been used as models to study the role of MYCN backgrounds[45] on tumor development and are in addition perfectly suited to examine the role of tumor cell- and stromal cell-derived CSF-1 in NB xenograft mouse models. Importantly, MYCN amplification occurs in about 22% of

NB cases[3] and sequential analysis of NB samples indicates that patients with no MYCN amplification at diagnosis rarely acquire it later during tumor progression.[3] Thus, other genetic and/or epigenetic alterations as well as tumor–host interactions may contribute to the pathogenesis of NB. Indeed, here we showed that genotypically distinct CSF-1-positive and -negative human NB cells express both host (mouse) CSF-1 and recruit TAMs to the tumor. We also showed that host CSF-1 blockade resulted in reduced TAM density and vessel infiltration in human NB xenografts in mice associated with suppression of tumor growth in both xenograft models. These findings suggest a key role for CSF-1-dependent TAMs in NB growth, because a similar reduction of tumor growth rate for both SK-N-AS and SK-N-DZ tumors is associated in both cases with a similar reduction in TAM density, angiogenesis and MMP-12 activity.

Our data show the presence of a Tie-2-positive TAM fraction in SK-N-AS NB tissue, comprising more than half of the TAMs. Moreover, the Tie-2-positive TAM fraction is to a large extent CSF-1 dependent. Recently, a distinct lineage of Tie-2-expressing monocytes (TEMs) has been identified, which has been shown to promote tumor vascularization.[46] Moreover, Venneri *et al.* have shown that Tie-2-expressing TAMs were observed within the tumors in human cancer patients, derived from Tie-2-expressing blood monocytes (TEMs).[47] Thus, we assume that the observed Tie-2-positive TAMs in NB tumor tissue are derived from circulating TEMs. However, although Venneri *et al.* reported that TEMs migrated toward the Tie-2 ligand angiopoietin-2 *in vitro*, suggesting a homing mechanism for TEMs to tumors, our data show for the first time that CSF-1 is able to recruite TEMs to NB tumors. Interestingly, purified human TEMs, but not Tie-2-depleted monocytes, markedly promote angiogenesis in xenotransplanted human tumors.[47] Thus, further investigations are necessary to clarify whether CSF-1-dependent TAMs in NB tumor tissue can be further subdivided into functionally different, *i.e.* proangiogenic and ECM-degrading/ growth factor-producing TAM subpopulations involved in NB growth.

Host expression of the specific angiogenic genes VEGF-A and KDR and increasing angiogenic activity during tumor development were suppressed following muCSF-1 siRNA treatment in both SK-N-AS and SK-N-DZ NB xenografts. With increasing host VEGF-A production during tumor growth in both NBs, human VEGF-A production decreased. CSF-1 has been shown to induce VEGF production and angiogenic activity by monocytes *in vitro*,[29] and *in vivo* studies indicated that the secretion of VEGF by TAMs is essential for tumor-induced angiogenesis.[48] In line with this, the coculture results showed host CSF-1-dependent upregulation of stromal cell-derived VEGF-A by both NB cell lines. These data therefore suggest that increased host VEGF-A production induced by interactions between TAM and fibroblast host cells and NB cancer cells is important for the angiogenic response in NB and may significantly contribute not only to tumor growth but also to the systemic destructive effects on multiple organs and tissues caused by tumor-produced VEGF observed in mice and cancer patients in the advanced stage of disease.[49]

The tissue inhibitors of MMPs (TIMPs) play a unique role in regulating tumorigenesis and angiogenesis. Overexpression of TIMP-3 in NB xenografts reduces vascular endothelial cadherin-mediated angiogenesis, resulting in decreased recruitment of pericytes to the tumor and the emergence of immature vasculature.[50] TIMP-3 also blocks the binding of VEGF to KDR, thereby inhibiting downstream signaling in angiogenesis.[51] It is therefore not surprising that stromal TIMP-3 deficiency was shown to inhibit tumorigenesis.[52] In addition, TIMP-2, the inhibitor of MMP-2, has been shown to inhibit angiogenesis through a mechanism that is independent of MMPs.[53] In our study, TIMP-3 was significantly upregulated by muCSF-1 siRNA treatment. This observation was surprising, because in our earlier studies on breast cancer,[15] TIMP-3 expression was not significantly changed after muCSF-1 siRNA treatment. However, as indicated in several studies,[42] NBs differ in their

behavior from other malignant cells. In addition to the TIMP-3 upregulation, TIMP-2 was upregulated following muCSF-1 blockade, although MMP-2 levels were not changed. The failure of NB cells to increase MMP-2 was also confirmed in coculture experiments using macrophages, fibroblasts and NB cells in which stromal cell-derived MMP-2 levels were unchanged. Thus, muCSF-1 siRNA treatment may increase levels of TIMPs to counteract MMP-2-independent NB-induced angiogenesis.

In contrast to similar reductions in tumor growth, NB cells differed in their proliferation *in vitro*, huVEGF-A production in vivo and animal survival responses to blockade of CSF-1. Mouse CSF-1 blockade increased the survival of mice bearing the CSF-1-negative SK-N-DZ tumors, in contrast to mice bearing the CSF-1-positive SK-N-AS tumors, where CSF-1 blockade did not prolong survival. The proliferation results *in vitro* demonstrated that cultured CSF-1-positive tumor cells failed to proliferate in response to CSF-1 or to be inhibited by huCSF-1R blockade, indicating that they were not dependent on CSF-1 for proliferation or survival. However, the growth of those tumors was more robust than the growth of the CSF-1-negative tumors (Fig. 3*a*), and despite their similar degree of growth inhibition by day 24, the survival of the mice was determined at a later time (>30 days). Factors such as the continued production of huCSF-1 (Fig. 1) and huVEGF-A (Fig. 6*b*), both of which are active on host cells, could have differentially increased macrophage accumulation and angiogenesis in the CSF-1-positive tumors after day 24 and thereby have overridden the effects of muCSF-1 blockade in increasing survival of the mice. Our macrophage migration assay findings showing significantly higher macrophage migration to cocultured SK-N-AS cells even following stromal cell-derived CSF-1 and VEGF-A inhibition in comparison to SKN-DZ cocultures support this assumption. Figure 7 schematically illustrates the regulation by CSF-1 in the CSF-1-positive and CSF-1-negative NB xenografts used in our study.

The failure of muCSF-1 blockade to increase survival of mice bearing the huCSF-1-positive tumors, in which there is no apparent autocrine regulation by CSF-1, is consistent with effects of tumor cell-derived huCSF-1 on host TAMs. In future experiments with CSF-1-producing human tumor xenografts, comparison of the simultaneous blockade of huCSF-1 and muCSF-1 with blockade by each alone could resolve the differential contributions of tumor- and host-derived CSF-1. This will be of interest in the event of therapeutic inhibition of CSF-1 in human disease.

Acknowledgments

The authors thank the members of the Center for Biomedical Research of the Vienna Medical University for helping with animal care and continuing support; and Friederike Schramm and Britta Klein for technical support. This work was supported by a grant from the Austrian Research Foundation (FWF; S9412-B11 to S.A.), European Commission (“Anti-tumor-targeting” LSHC-CT-2005-518178 to S.A.), Norwegian Cancer Society (to M.S.) and National Institutes of Health (CA 26504 and PO1 CA 100324 to E.R.S.).

Grant sponsor: Austrian Research Foundation; **Grant number:** FWF S9412-B11; **Grant sponsor:** European Commission; **Grant number:** LSHC-CT-2005-518178; **Grant sponsor:** National Institutes of Health; **Grant numbers:** CA 26504 and PO1 CA 100324; **Grant sponsor:** Norwegian Cancer Society

Abbreviations

CSF-1	colony-stimulating factor-1
CSF-1R	CSF-1 receptor
DAPI	4′-6-diamidino-2-phenylindole
EC	endothelial cell

ECM	extracellular matrix
MMP	matrix metalloprotease
NB	neuroblastoma
RIA	radioimmunoassay
siRNA	small interfering RNAs
TAM	tumor-associated macrophage
TEM	Tie-2-expressing monocytes
TIMPs	tissue inhibitors of MMPs
VEGF	vascular endothelial growth factor

References

1. Brodeur, G.; Maris, J. Neuroblastoma.. In: Pizzo, P.; Poplack, DG., editors. Cytokine reference. 4th edn.. Academic press; London: 2002. p. 895-938.
2. van Noesel MM, Versteeg R. Pediatric neuroblastomas: genetic and epigenetic 'danse macabre.'. Gene. 2004; 325:1–15. [PubMed: 14697505]
3. Brodeur GM. Neuroblastoma: biological insights into a clinical enigma. Nat Rev Cancer. 2003; 3:203–16. [PubMed: 12612655]
4. Goldsmith KC, Hogarty MD. Targeting programmed cell death pathways with experimental therapeutics: opportunities in high-risk neuroblastoma. Cancer Lett. 2005; 228:133–41. [PubMed: 15927359]
5. Nilsson JA, Keller UB, Baudino TA, Yang C, Norton S, Old JA, Nilsson LM, Neale G, Kramer DL, Porter CW, Cleveland JL. Targeting ornithine decarboxylase in Myc-induced lymphomagenesis prevents tumor formation. Cancer Cell. 2005; 7:433–44. [PubMed: 15894264]
6. Maris JM, Hogarty MD, Bagatell R, Cohn SL. Neuroblastoma. Lancet. 2007; 369:2106–20. [PubMed: 17586306]
7. Wang Q, Diskin S, Rappaport E, Attiyeh E, Mosse Y, Shue D, Seiser E, Jagannathan J, Shusterman S, Bansal M, Khazi D, Winter C, et al. Integrative genomics identifies distinct molecular classes of neuroblastoma and shows that multiple genes are targeted by regional alterations in DNA copy number. Cancer Res. 2006; 66:6050–62. [PubMed: 16778177]
8. Eggert A, Ikegaki N, Kwiatkowski J, Zhao H, Brodeur GM, Himelstein BP. High-level expression of angiogenic factors is associated with advanced tumor stage in human neuroblastomas. Clin Cancer Res. 2000; 6:1900–8. [PubMed: 10815914]
9. Nissen LJ, Cao R, Hedlund EM, Wang Z, Zhao X, Wetterskog D, Funa K, Brakenhielm E, Cao Y. Angiogenic factors FGF2 and PDGF-BB synergistically promote murine tumor neovascularization and metastasis. J Clin Invest. 2007; 117:2766–77. [PubMed: 17909625]
10. Cao R, Bjorndahl MA, Religa P, Clasper S, Garvin S, Galter D, Meister B, Ikomi F, Tritsaris K, Dissing S, Ohhashi T, Jackson DG, et al. PDGF-BB induces intratumoral lymphangiogenesis and promotes lymphatic metastasis. Cancer Cell. 2004; 6:333–45. [PubMed: 15488757]
11. Palmberg E, Johnsen JI, Paulsson J, Gleissman H, Wickstrom M, Edgren M, Ostman A, Kogner P, Lindskog M. Metronomic scheduling of imatinib abrogates clonogenicity of neuroblastoma cells and enhances their susceptibility to selected chemotherapeutic drugs in vitro and in vivo. Int J Cancer. 2009; 124:1227–34. [PubMed: 19058199]
12. Pollard JW. Tumour-educated macrophages promote tumour progression and metastasis. Nat Rev Cancer. 2004; 4:71–8. [PubMed: 14708027]
13. Cao Y. Opinion: emerging mechanisms of tumour lymphangiogenesis and lymphatic metastasis. Nat Rev Cancer. 2005; 5:735–43. [PubMed: 16079909]

14. Aharinejad S, Abraham D, Paulus P, Abri H, Hofmann M, Grossschmidt K, Schafer R, Stanley ER, Hofbauer R. Colony-stimulating factor-1 antisense treatment suppresses growth of human tumor xenografts in mice. Cancer Res. 2002; 62:5317–24. [PubMed: 12235002]
15. Aharinejad S, Paulus P, Sioud M, Hofmann M, Zins K, Schafer R, Stanley ER, Abraham D. Colony-stimulating factor-1 blockade by antisense oligonucleotides and small interfering RNAs suppresses growth of human mammary tumor xenografts in mice. Cancer Res. 2004; 64:5378–84. [PubMed: 15289345]
16. Paulus P, Stanley ER, Schafer R, Abraham D, Aharinejad S. Colony-stimulating factor-1 antibody reverses chemoresistance in human MCF-7 breast cancer xenografts. Cancer Res. 2006; 66:4349–56. [PubMed: 16618760]
17. Zins K, Abraham D, Sioud M, Aharinejad S. Colon cancer cell-derived tumor necrosis factor-alpha mediates the tumor growth-promoting response in macrophages by up-regulating the colony-stimulating factor-1 pathway. Cancer Res. 2007; 67:1038–45. [PubMed: 17283136]
18. Condeelis J, Pollard JW. Macrophages: obligate partners for tumor cell migration, invasion, and metastasis. Cell. 2006; 124:263–6. [PubMed: 16439202]
19. Lewis CE, Pollard JW. Distinct role of macrophages in different tumor microenvironments. Cancer Res. 2006; 66:605–12. [PubMed: 16423985]
20. Mantovani A, Bottazzi B, Colotta F, Sozzani S, Ruco L. The origin and function of tumor-associated macrophages. Immunol Today. 1992; 13:265–70. [PubMed: 1388654]
21. Wyckoff J, Wang W, Lin EY, Wang Y, Pixley F, Stanley ER, Graf T, Pollard JW, Segall J, Condeelis J. A paracrine loop between tumor cells and macrophages is required for tumor cell migration in mammary tumors. Cancer Res. 2004; 64:7022–9. [PubMed: 15466195]
22. Ingber DE, Folkman J. How does extracellular matrix control capillary morphogenesis? Cell. 1989; 58:803–5. [PubMed: 2673531]
23. Stetler-Stevenson WG. Matrix metalloproteinases in angiogenesis: a moving target for therapeutic intervention. J Clin Invest. 1999; 103:1237–41. [PubMed: 10225966]
24. Polverini PJ. How the extracellular matrix and macrophages contribute to angiogenesis-dependent diseases. Eur J Cancer. 1996; 32A:2430–7. [PubMed: 9059331]
25. Sherr CJ, Rettenmier CW, Sacca R, Roussel MF, Look AT, Stanley ER. The c-fms proto-oncogene product is related to the receptor for the mononuclear phagocyte growth factor. CSF-1. Cell. 1985; 41:665–76. [PubMed: 2408759]
26. Chitu V, Stanley ER. Colony-stimulating factor-1 in immunity and inflammation. Curr Opin Immunol. 2006; 18:39–48. [PubMed: 16337366]
27. Pixley FJ, Stanley ER. CSF-1 regulation of the wandering macrophage: complexity in action. Trends Cell Biol. 2004; 14:628–38. [PubMed: 15519852]
28. Aharinejad S, Marks SC Jr, Bock P, Mason-Savas A, MacKay CA, Larson EK, Jackson ME, Luftensteiner M, Wiesbauer E. CSF-1 treatment promotes angiogenesis in the metaphysis of osteopetrotic (toothless, tl) rats. Bone. 1995; 16:315–24. [PubMed: 7540405]
29. Eubank TD, Galloway M, Montague CM, Waldman WJ, Marsh CB. M-CSF induces vascular endothelial growth factor production and angiogenic activity from human monocytes. J Immunol. 2003; 171:2637–43. [PubMed: 12928417]
30. Goswami S, Sahai E, Wyckoff JB, Cammer M, Cox D, Pixley FJ, Stanley ER, Segall JE, Condeelis JS. Macrophages promote the invasion of breast carcinoma cells via a colony-stimulating factor-1/epidermal growth factor paracrine loop. Cancer Res. 2005; 65:5278–83. [PubMed: 15958574]
31. Stanley ER. The macrophage colony-stimulating factor, CSF-1. Methods Enzymol. 1985; 116:564–87. [PubMed: 3003518]
32. Sorensen DR, Leirdal M, Sioud M. Gene silencing by systemic delivery of synthetic siRNAs in adult mice. J Mol Biol. 2003; 327:761–6. [PubMed: 12654261]
33. Sioud M. Therapeutic siRNAs. Trends Pharmacol Sci. 2004; 25:22–8. [PubMed: 14723975]
34. Liu SQ, Saijo K, Todoroki T, Ohno T. Induction of human autologous cytotoxic T lymphocytes on formalin-fixed and paraffin-embedded tumour sections. Nat Med. 1995; 1:267–71. [PubMed: 7585045]
35. Das SK, Stanley ER. Structure–function studies of a colony stimulating factor (CSF-1). J Biol Chem. 1982; 257:13679–84. [PubMed: 6982897]

36. Roussel MF, Downing JR, Rettenmier CW, Sherr CJ. A point mutation in the extracellular domain of the human CSF-1 receptor (c-fms proto-oncogene product) activates its transforming potential. Cell. 1988; 55:979–88. [PubMed: 2974321]
37. Lin EY, Nguyen AV, Russell RG, Pollard JW. Colony-stimulating factor 1 promotes progression of mammary tumors to malignancy. J Exp Med. 2001; 193:727–40. [PubMed: 11257139]
38. Litwin S, Lagadari M, Barrientos G, Roux ME, Margni R, Miranda S. Comparative immunohistochemical study of M-CSF and G-CSF in feto-maternal interface in a multiparity mouse model. Am J Reprod Immunol. 2005; 54:311–20. [PubMed: 16212652]
39. Abraham D, Hofbauer R, Schafer R, Blumer R, Paulus P, Miksovsky A, Traxler H, Kocher A, Aharinejad S. Selective downregulation of VEGF-A(165), VEGFR(1), and decreased capillary density in patients with dilative but not ischemic cardiomyopathy. Circ Res. 2000; 87:644–7. [PubMed: 11029398]
40. Bartocci A, Pollard JW, Stanley ER. Regulation of colony-stimulating factor 1 during pregnancy. J Exp Med. 1986; 164:956–61. [PubMed: 3489064]
41. Shipley JM, Wesselschmidt RL, Kobayashi DK, Ley TJ, Shapiro SD. Metalloelastase is required for macrophage-mediated proteolysis and matrix invasion in mice. Proc Natl Acad Sci USA. 1996; 93:3942–6. [PubMed: 8632994]
42. Ribatti D, Marimpietri D, Pastorino F, Brignole C, Nico B, Vacca A, Ponzoni M. Angiogenesis in neuroblastoma. Ann N Y Acad Sci. 2004; 1028:133–42. [PubMed: 15650239]
43. Tang XX, Zhao H, Kung B, Kim DY, Hicks SL, Cohn SL, Cheung NK, Seeger RC, Evans AE, Ikegaki N. The MYCN enigma: significance of MYCN expression in neuroblastoma. Cancer Res. 2006; 66:2826–33. [PubMed: 16510605]
44. Zaizen Y, Taniguchi S, Noguchi S, Suita S. The effect of N-myc amplification and expression on invasiveness of neuroblastoma cells. J Pediatr Surg. 1993; 28:766–9. [PubMed: 8331499]
45. Marcus K, Johnson M, Adam RM, O'Reilly MS, Donovan M, Atala A, Freeman MR, Soker S. Tumor cell-associated neuropilin-1 and vascular endothelial growth factor expression as determinants of tumor growth in neuroblastoma. Neuropathology. 2005; 25:178–87. [PubMed: 16193833]
46. De Palma M, Venneri MA, Galli R, Sergi L, Politi LS, Sampaolesi M, Naldini L. Tie2 identifies a hematopoietic lineage of proangiogenic monocytes required for tumor vessel formation and a mesenchymal population of pericyte progenitors. Cancer Cell. 2005; 8:211–26. [PubMed: 16169466]
47. Venneri MA, De Palma M, Ponzoni M, Pucci F, Scielzo C, Zonari E, Mazzieri R, Doglioni C, Naldini L. Identification of proangiogenic TIE2-expressing monocytes (TEMs) in human peripheral blood and cancer. Blood. 2007; 109:5276–85. [PubMed: 17327411]
48. Barbera-Guillem E, Nyhus JK, Wolford CC, Friece CR, Sampsel JW. Vascular endothelial growth factor secretion by tumor-infiltrating macrophages essentially supports tumor angiogenesis, and IgG immune complexes potentiate the process. Cancer Res. 2002; 62:7042–9. [PubMed: 12460925]
49. Xue Y, Religa P, Cao R, Hansen AJ, Lucchini F, Jones B, Wu Y, Zhu Z, Pytowski B, Liang Y, Zhong W, Vezzoni P, et al. Anti-VEGF agents confer survival advantages to tumor-bearing mice by improving cancer-associated systemic syndrome. Proc Natl Acad Sci USA. 2008; 105:18513–18. [PubMed: 19017793]
50. Spurbeck WW, Ng CY, Strom TS, Vanin EF, Davidoff AM. Enforced expression of tissue inhibitor of matrix metalloproteinase-3 affects functional capillary morphogenesis and inhibits tumor growth in a murine tumor model. Blood. 2002; 100:3361–8. [PubMed: 12384438]
51. Qi JH, Ebrahem Q, Moore N, Murphy G, Claesson-Welsh L, Bond M, Baker A, Anand-Apte B. A novel function for tissue inhibitor of metalloproteinases-3 (TIMP3): inhibition of angiogenesis by blockage of VEGF binding to VEGF receptor-2. Nat Med. 2003; 9:407–15. [PubMed: 12652295]
52. Cruz-Munoz W, Kim I, Khokha R. TIMP-3 deficiency in the host, but not in the tumor, enhances tumor growth and angiogenesis. Oncogene. 2006; 25:650–5. [PubMed: 16186800]
53. Stetler-Stevenson WG, Seo DW. TIMP-2: an endogenous inhibitor of angiogenesis. Trends Mol Med. 2005; 11:97–103. [PubMed: 15760767]

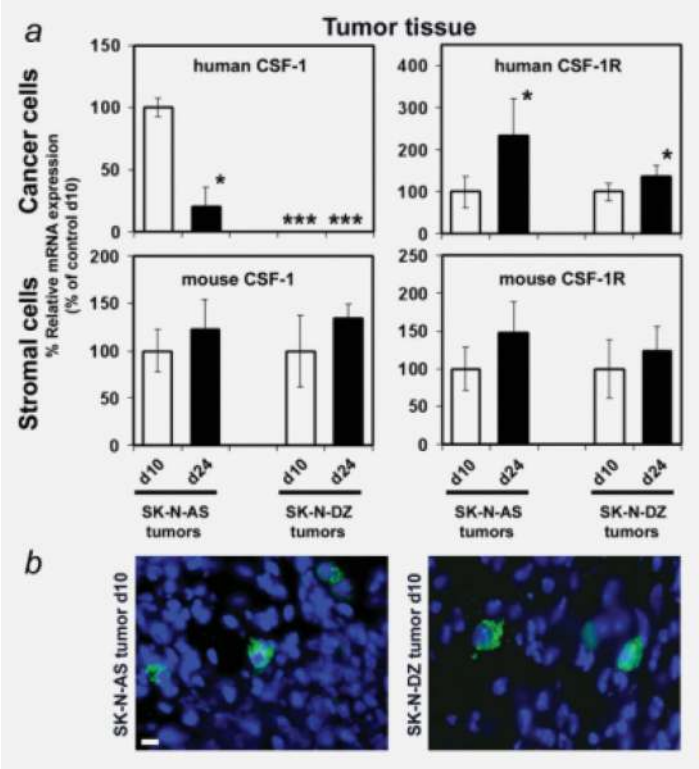

Figure 1.

(*a*) CSF-1 and CSF-1 receptor expression changes in the growing tumor. Quantitative RT-PCR mRNA measurements of human CSF-1, human CSF-1R, mouse CSF-1 and mouse CSF-1R in SK-N-AS and SK-N-DZ tumor lysates were performed on days 10 and 24 following tumor cell xenografting. *, Significantly different from tumor on day 10 (d10; SK-N-AS, $p < 0.001$; SK-N-DZ, $p < 0.01$); ***, mRNA not detectable. (*b*) Representative immunohistochemical images of SK-N-AS (left) and SK-N-DZ (right) day 10 tumor tissue sections stained with antibody against mouse CSF-1. Alexa-488 fluorescence indicates mouse (host) CSF-1-positive stromal cells. Nuclei are counterstained with DAPI (scale bar: 10 μm).

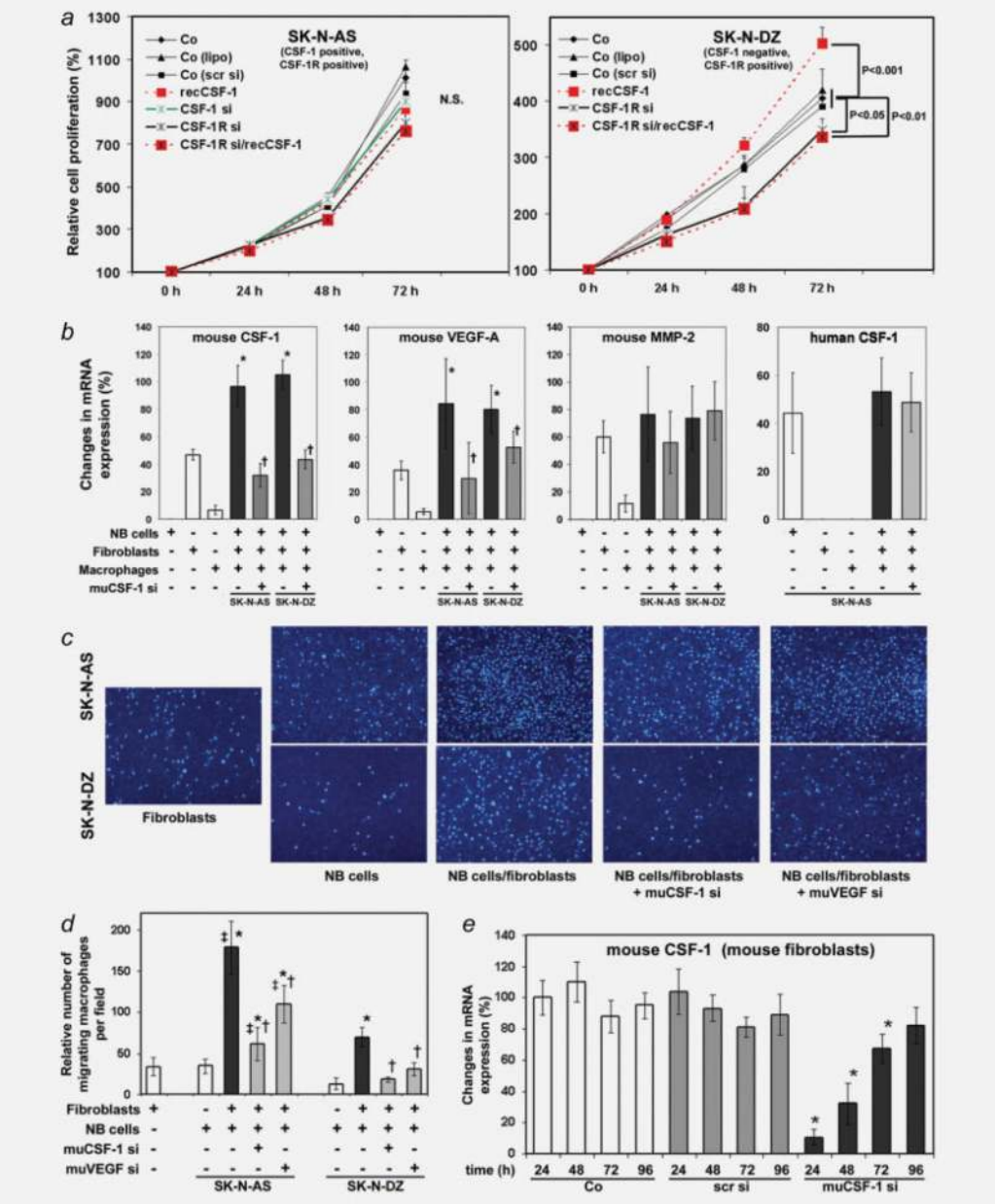

Figure 2.

(*a*) Effects of CSF-1 and CSF-1R on SK-N-AS and SK-N-DZ cell proliferation. Relative cell densities of NB cells up to 72 hr following treatment with recombinant huCSF-1 (recCSF-1), siRNA against huCSF-1 (CSF-1 si) and huCSF-1R (CSF-1R si) and a combination of huCSF-1R siRNA (CSF-1R si) and recombinant huCSF-1 (recCSF-1) were measured using the WST-1 reagent. Control cells (Co) were untreated, treated with Lipofectamine (lipo) or scrambled siRNA (scr-si). *, $p < 0.01$, significantly different from control (co). (*b*) Cancer cell–stromal cell interactions upregulate stromal cell gene expression. SK-N-AS or SK-N-DZ cancer cells were cocultured with mouse CRL-2470 macrophages and mouse S3T3 fibroblasts. Mouse CSF-1, VEGF-A, MMP-2 and human CSF-1 mRNA expression were measured by real-time RT-PCR in RNA from cultured cells alone or from cocultured human NB cancer cells and mouse macrophages and fibroblasts following treatment with or without mouse CSF-1 siRNA (muCSF-1-si). Results were

normalized to human and mouse β-2 microglobulin mRNA levels, respectively, and expressed as relative changes in mRNA expression (mean ± SD). *, Significantly different from cultured mouse fibroblasts and macrophages ($p < 0.001$); †, Significantly different from cocultured NB cells, fibroblasts and macrophages ($p < 0.001$ for mouse CSF-1 and $p < 0.01$ for mouse VEGF-A). (*c, d*) Fibroblast-derived CSF-1 and VEGF-A promote macrophage migration. Representative images (*c*) and quantification (*d*) of migrated macrophages from an *in vitro* migration assay. Macrophage cell migration to cultured fibroblasts, SK-N-AS or SK-N-DZ NB cells or cocultured NB cells/fibroblasts treated with or without muCSF-1 siRNA (muCSF-1 si) and siRNA against mouse VEGF-A (muVEGF si) was measured in a Boyden incubation chamber. Data were collected from 5 individual consecutive fields of view (×10) from 3 replicate Boyden chambers. *, Significantly different from cultured fibroblasts and NB cells ($p < 0.001$); †, Significantly different from cocultured NB cells/fibroblasts ($p < 0.001$) ‡, significantly different from SK-N-DZ cocultures ($p < 0.001$). (*e*) siRNA directed against mouse CSF-1 down-regulates target gene expression in mouse S3T3 fibroblasts as determined in cell lysates by real-time reverse transcription-PCR. CSF-1 mRNA expression decreases significantly up to 72 hr following treatment with 100 nM mouse CSF-1 siRNA (muCSF-1 si) as compared to scrambled siRNA (scr si) and untreated control (Co). *, Significantly different from controls and scrambled siRNA ($p < 0.001$ for 24 and 48 hr and $p = 0.016$ for 72 hr).

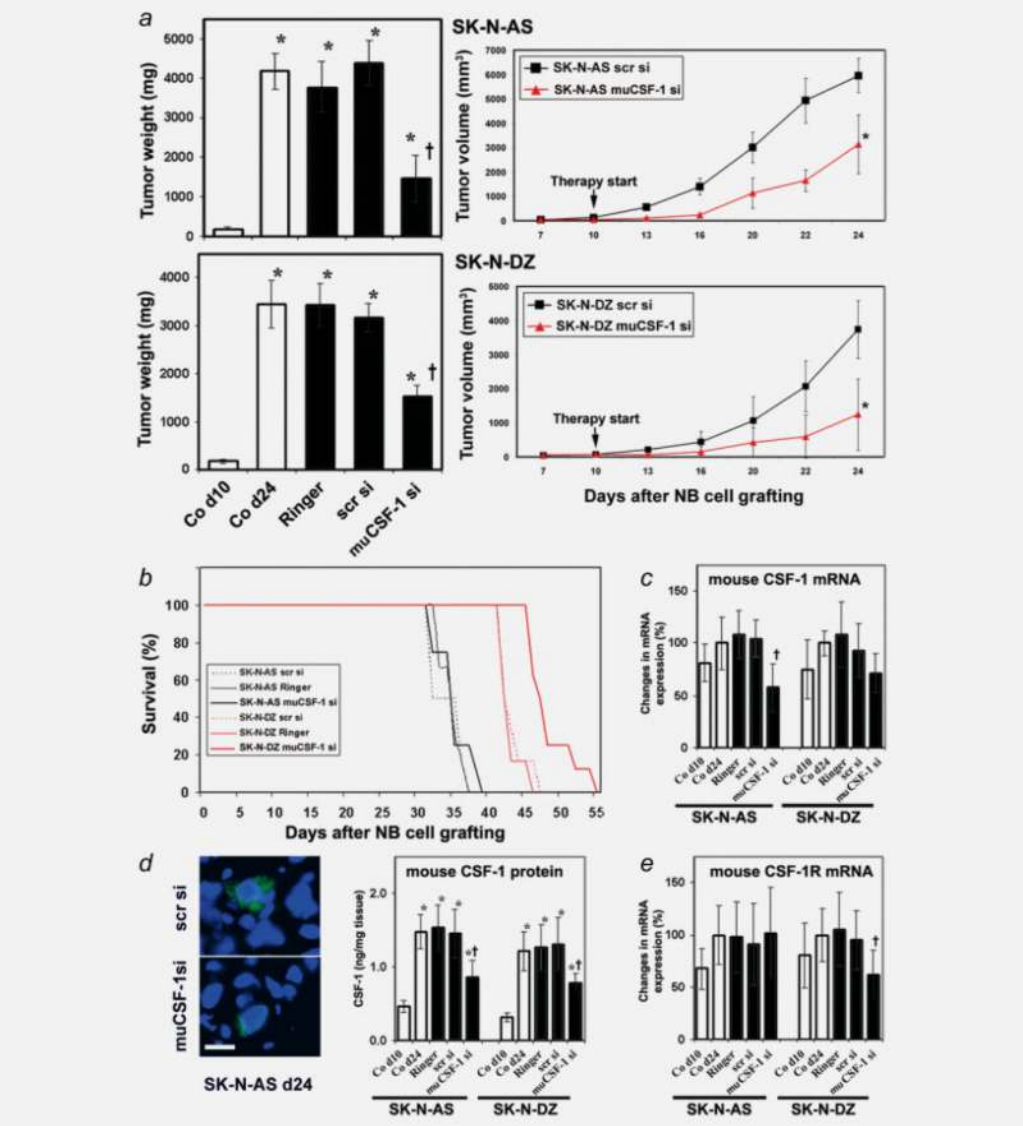

Figure 3.

muCSF-1 siRNAs suppresses NB growth in mice. (*a*) Left panel: mean NB xenograft weights of human SK-N-AS (upper histogram) and SK-N-DZ NB (lower histogram) xenografts in control mice on day 10 (Co d10; therapy start), in control mice on day 24 (Co d24; therapy end), in control mice treated with Ringer's solution on day 24 (Ringer) and in mice treated with scrambled siRNA (scr si), or muCSF-1 siRNA (muCSF-1 si). *, Significantly different from Co d10 ($p < 0.001$); †, Significantly different from Co d24, Ringer and scr si ($p < 0.001$). Right panel: tumor volume of SK-N-AS and SK-N-DZ NB xenografts in control mice (treated with scrambled siRNA; scr si) and in mice treated with muCSF-1 siRNA (muCSF-1 si) from day 7 to day 24. *, Significantly different from scr si ($p < 0.001$); ***, not detectable. (*b*) Survival of mice with NB xenografts. Survival is increased significantly in SK-N-DZ-bearing mice after treatment with muCSF-1 siRNA (SK-N-DZ muCSF-1 si; $p = 0.002$ and $p = 0.004$ *vs.* Ringer's solution-treated [SK-N-DZ Ringer] and scrambled siRNA-treated [SK-N-DZ scr si] mice, respectively), but not in SK-N-AS bearing mice vs. control animals. At day 46, when the last animal of the SK-N-DZ control group had died, 50% of the muCSF-1 siRNA-treated mice were still alive. (*c–e*)

muCSF-1 siRNA downregulates expression of target molecules *in vivo*. (*c*) Quantitative muCSF-1 mRNA measurements by real-time RT-PCR. (*d*) Left panel: representative immunohistochemical images of SK-N-AS day 24 tumor tissue sections stained with antibody against mouse CSF-1. Alexa-488 fluorescence indicates mouse (host) CSF-1-positive stromal cells. Nuclei are counterstained with DAPI (scale bar: 10 μm); right panel: quantitative protein measurements by muCSF-1 RIA. (*e*) Quantitative RT-PCR measurements of muCSF-1R mRNA in tumor lysates of mice xenografted with SK-N-AS and SK-N-DZ NB cells. *, Significantly different from Co d10 ($p < 0.003$ in panel *a*; $p < 0.005$ in panel *d*); †, Significantly different from Co d24, Ringer and scr si ($p = 0.005$ in panel *a*; $p < 0.009$ in panel *c*; and $p < 0.03$ in panels *d* and *e*).

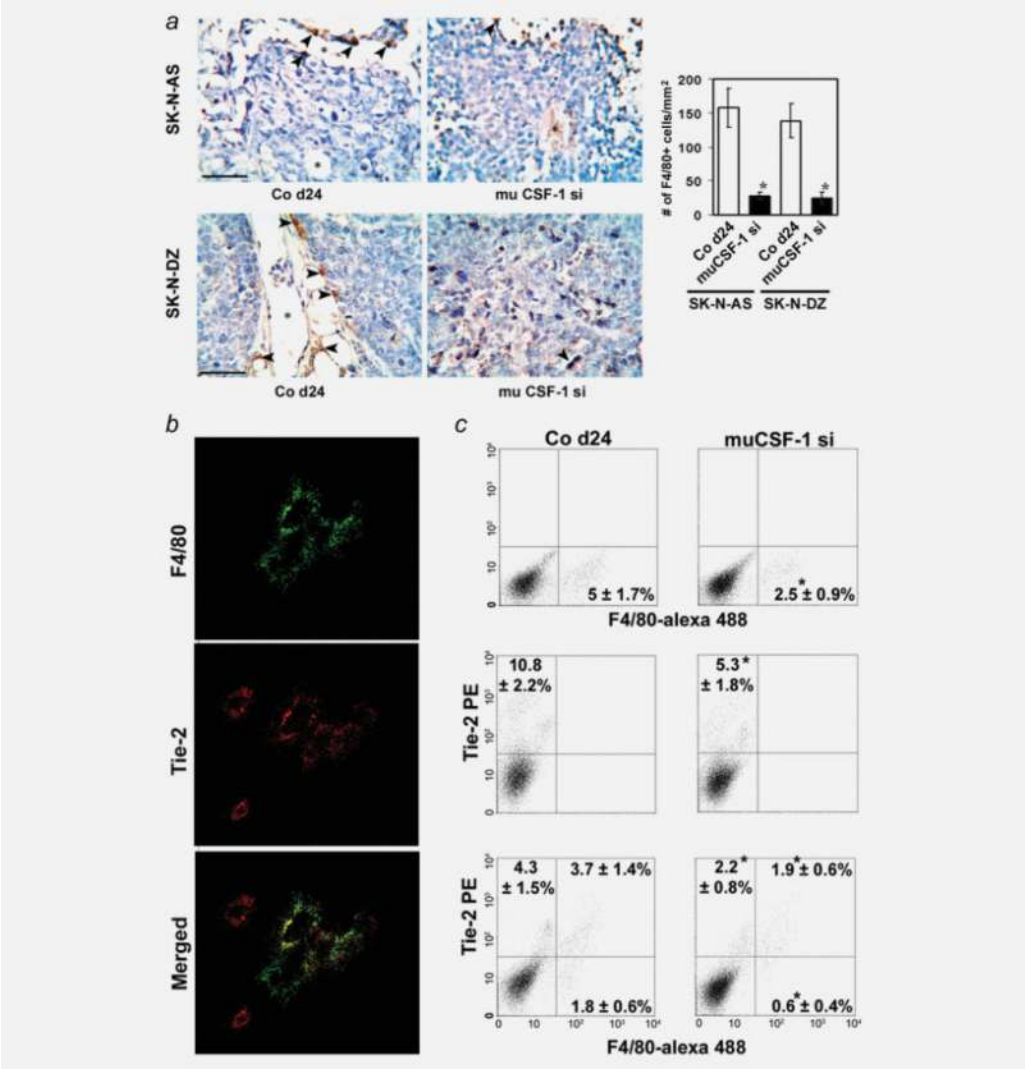

Figure 4.

Invasion of Tie-2-positive and -negative macrophages is reduced by host CSF-1 blockade in SK-N-AS and SK-N-DZ NB xenografts. (*a*) Left panels: representative immunohistochemistry images of tumor tissue sections in a control mouse on day 24 (Co d24) and in mice treated with muCSF-1 siRNA (muCSF-1 si) stained with antibody to the mouse macrophage marker protein F4/80. Arrows indicate TAMs staining positively with F4/80 antibody that lines vascular channels (asterisk), some of which contain blood cells. Calibration bar = 50 μm. Right panel: results of a quantitative histomorphometric analysis showing the density of F4/80-positive cells. *, Significantly different from Co d24 ($p < 0.001$). (*b*) Localization of TAMs and endothelial cells in SK-N-AS NB xenografts. Confocal images of cells immunostained with anti-F4/80 rat monoclonal antibody specific for macrophages (green fluorescence), or with anti-Tie-2 (red fluorescence). An overlay of F4/80 and Tie-2 staining shows localization of F4/80 cells to blood vessels as well as colocalization of F4/80 and Tie-2, indicating that Tie-2-positive macrophages line the tumor vessels. Also shown are areas that stain with Tie-2 alone, outlining endothelial cell-lined vessels. Scale bar = 50 μm. (*c*) Representative images and quantification of the number of F4/80- and Tie-2-positive cells in day 24 SK-N-AS NB tissue from the untreated control group (left panels) and from mice treated with anti-mouse CSF-1 si RNA (muCSF-1si)

(right panels). Total F4/80-positive (upper panel) and Tie-2-positive (middle panel) cells as well as Tie-2-positive and Tie-2-negative F4/80-positive macrophage subpopulations were determined using flow cytometric analysis. *, Significantly different from Co d24 ($p < 0.048$).

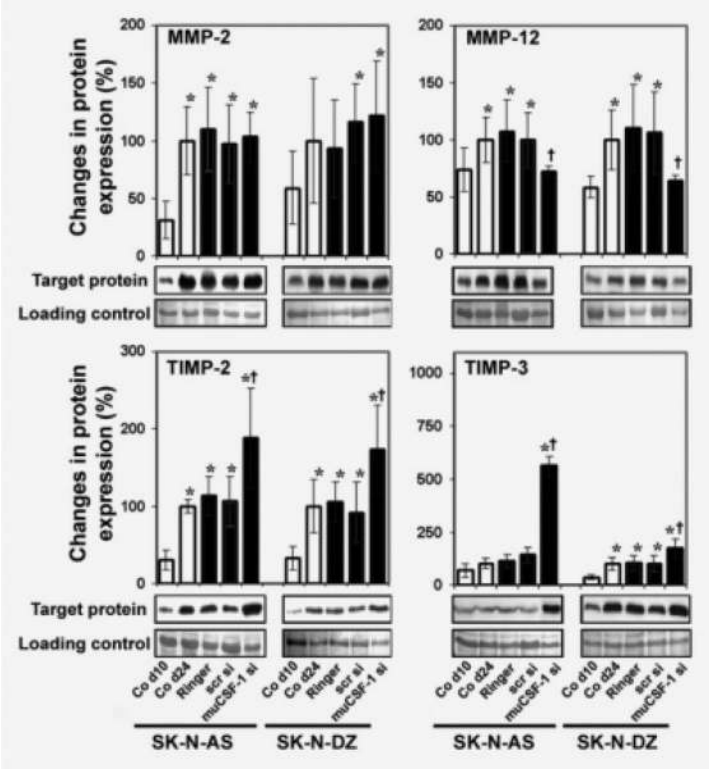

Figure 5.

muCSF-1 blockade reduces MMP-12 expression and increases expression of TIMPs in SK-N-AS and SK-N-DZ NB xenografts. Representative western blot images, together with the data for quantitative determination of protein expression in tumor lysates of MMP-2 and -12 (upper panels) and TIMP-2 and -3 (lower panels) for control mice on days 10 (Co d10) and 24 (Co d24) and in mice treated with Ringer's solution (Ringer), scrambled siRNA (scr si) or muCSF-1 siRNA (muCSF-1 si). *, Significantly different from Co d10 ($p < 0.022$ in MMP-2, $p < 0.02$ in MMP-12, $p < 0.013$ in TIMP-2, $p < 0.005$ in TIMP-3); †, significantly different from Co d24, Ringer and scr si ($p < 0.015$ in MMP-12, $p < 0.007$ in TIMP-2, $p < 0.001$ in TIMP-3).

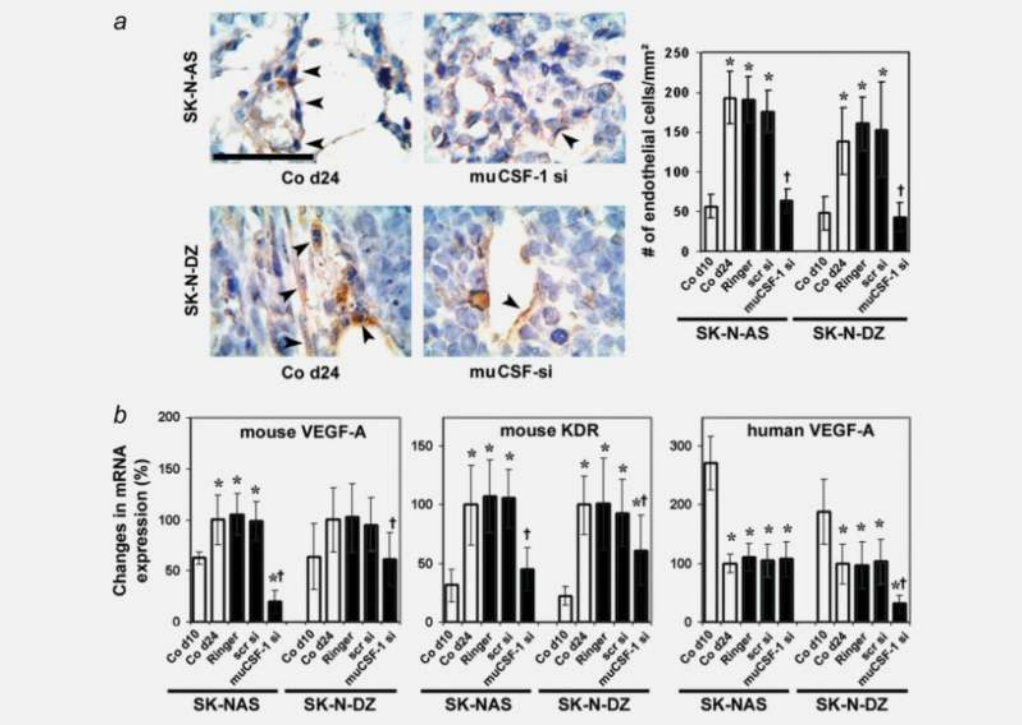

Figure 6.

Angiogenic activity in SK-N-AS and SK-N-DZ NB tumor xenografts is decreased by muCSF-1 blockade. (*a*) Representative immunocytochemical images of vWF-stained tumor tissue sections in control mice on day 24 (Co d24) and in mice treated with muCSF-1 siRNA (muCSF-1 si) (left panels) together with quantification of vWF-positive ECs (right panel). Arrowheads indicate vWF-positive cells. *, Significantly different from control on day 10 (Co d10; $p < 0.001$; †, significantly different from Co d24, Ringer and scr si, $p < 0.001$). Scale bar = 100 μm. (*b*) Quantitative RT-PCR measurements of mRNA of mouse VEGF-A, mouse VEGF-A receptor KDR and human VEGF-A in tumor lysates. *, Significantly different from control on day 10 (Co d10; $p < 0.047$ in mouse VEGF-A, $p < 0.03$ in KDR and $p < 0.001$ in human VEGF-A); †, significantly different from Co d24, Ringer and scr si ($p < 0.036$ in mouse VEGF-A, $p < 0.007$ in KDR and $p < 0.006$ in human VEGF-A).

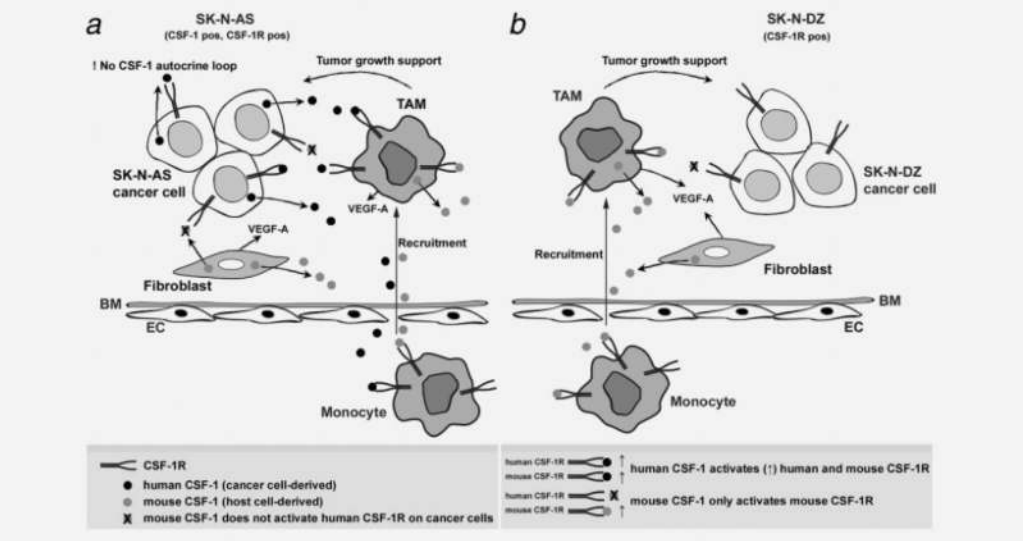

Figure 7.

Proposed model for the role of host and cancer cell-derived CSF-1-regulated tumor development in SK-N-AS and SK-N-DZ NB. (*a*) SK-N-AS tumor model. A subset of circulating monocytes transverse the basement membrane (BM) and endothelium (ENDO) and migrate to the tumor as tumor-associated macrophages (TAMs). TAM recruitment is promoted by host CSF-1 and VEGF-A derived from TAMs and stromal cells (fibroblasts) and (human) CSF-1 derived from tumor cells. TAMs then support tumor growth and invasion by secretion of growth factors and extracellular matrix modifying factors. Stromal cell-derived (mouse) CSF-1 does not activate human CSF-1R on cancer cells. (*b*) SK-N-DZ tumor model. A subset of circulating monocytes transverse the BM and ENDO and migrate to the tumor as TAMs. TAM recruitment is promoted by host CSF-1 and VEGF-A derived from TAMs and stromal cells (fibroblasts). TAMs then support tumor growth and invasion by secretion of growth factors and extracellular matrix modifying factors, highlighting the importance of host CSF-1 in this model. There is no human CSF-1 autocrine loop in SK-N-DZ tumor cells.